

# Hydrogenation of Dicyclopentadiene in the Presence of a Nickel Catalyst Supported onto a Cation Exchanger in a Flow-Type Reactor

Yu. V. Popov<sup>a, \*</sup>, V. M. Mokhov<sup>a</sup>, D. N. Nebykov<sup>a</sup>, S. E. Latyshova<sup>a</sup>,  
K. V. Shcherbakova<sup>a</sup>, and A. O. Panov<sup>a</sup>

<sup>a</sup>Volgograd State Technical University, Volgograd, 400131 Russia

\*e-mail: tons@vstu.ru

Received April 6, 2017

**Abstract**—The process of dicyclopentadiene hydrogenation in the gas–liquid–solid catalyst system with a catalyst of nickel nanoparticles supported onto a Purolite CT-175 cation exchange resin was studied. The surface structure of the catalyst and the kinetics of the dicyclopentadiene hydrogenation process were examined. Optimum conditions were found for the production of *endo*-tetrahydrodicyclopentadiene and the simultaneous production of *endo*-tetrahydrodicyclopentadiene and 5,6-dihydrodicyclopentadiene at atmospheric pressure.

**Keywords:** hydrogenation, dicyclopentadiene, nanosized nickel catalyst

**DOI:** 10.1134/S0023158418040109

## INTRODUCTION

Dicyclopentadiene as a by-product in the manufacture of ethylene and propylene by the high-temperature pyrolysis of petroleum fractions is an important intermediate in industrial chemical synthesis. It is used for the production of adamantane and its derivatives and in the manufacture of pesticides, ternary ethylene–propylene rubbers, hydraulic fluids, rubber antioxidants, and the components of perfume compositions [1]. An important line in the application of dicyclopentadiene is the production of high-energy rocket propellants based on the *exo* isomer of tetrahydrodicyclopentadiene. This isomer is obtained by the hydrogenation of dicyclopentadiene to *endo*-tetrahydrodicyclopentadiene with the subsequent isomerization [2].

However, the process of dicyclopentadiene hydrogenation requires either severe process conditions with the use of available nickel catalysts or the use of highly active and selective catalysts based on expensive metals (platinum, palladium, iridium, and rhodium). For example, the hydrogenation of dicyclopentadiene on a Pd/Al<sub>2</sub>O<sub>3</sub> catalyst is conducted at a temperature to 165°C and a pressure to 30 atm in a stirred batch reactor for 40–60 min with a product yield to 90% with a catalyst load about 0.6 g per 0.27 mol of dicyclopentadiene [3].

The application of nanosized catalysts is a method for improving dicyclopentadiene hydrogenation technologies. The catalysts of this kind, which possess quantitatively and qualitatively new properties, make it

possible to considerably intensify the chemical processes that occur in their presence and to increase their energy efficiency. In particular, it was found that the hydrogenation of dicyclopentadiene on the nanoparticles of palladium can be performed in a stirred batch reactor at 60°C and a hydrogen pressure of 5 atm for 2 h with a yield of ~50% at a catalyst load of about 0.31 mg per 0.028 mol of dicyclopentadiene [4]. The catalysts based on the nanoparticles of noble metals—platinum, palladium, ruthenium, and rhodium—are most commonly used for the heterogeneous catalytic processes of the hydrogenation of unsaturated hydrocarbons [5–8]. For increasing the stability of the nanoparticles, they are supported onto different carriers, in particular, aluminum oxide, silicon oxide, activated carbon, barium sulfate, and calcium carbonate [9–13].

We developed a method for the hydrogenation of alkenes, cycloalkenes, and unsaturated aromatic hydrocarbons in a gas phase in a continuous flow reactor with the fixed bed of a nanocatalyst of nickel nanoparticles supported on zeolite A. Thus, for instance, *endo*-tetrahydrodicyclopentadiene was obtained with a yield of 98% (180°C; a fivefold or sixfold excess of H<sub>2</sub> at atmospheric pressure) [14].

Within the framework of this study, we were the first to use the submicro- and nanoparticles of nickel stabilized on the surface of a Purolite CT-175 cation exchange resin (CER) carrier as a catalyst for the hydrogenation of dicyclopentadiene [15]. In comparison with other carriers (zeolites, silica gel, aluminum

oxide, and activated carbon), ion-exchange resins as the carriers of nanoparticles have a number of advantages: the possibility of nanoparticle stabilization due to charged functional groups and porosity, commercial availability, satisfactory chemical, mechanical, and thermal stability, and convenient transportation and regeneration [16].

## EXPERIMENTAL

The catalyst was obtained by the impregnation of a cation exchange resin (Purolite CT-175,  $m_{\text{CER}} = 0.5$  g) with an aqueous solution of nickel(II) chloride hexahydrate ( $m_{\text{NiCl}_2 \cdot 6\text{H}_2\text{O}} = 0.3$  g, 2.5 mL of water) for 24 h with the subsequent filtration and washing with distilled water. Then, adsorbed nickel was reduced by sodium tetrahydroborate ( $m_{\text{NaBH}_4} = 0.1$  g) in 2.5 mL of water at 20–25°C for 30 min.

The mass concentration of nickel was determined by photocolometry on a Shimadzu UV-1800 spectrophotometer (Shimadzu, Japan). It was found that the Ni<sup>0</sup>/CER catalyst contained 6.7 wt % nickel.

A FEI Versa 3D DualBeam instrument (FEI, the United States) was used for scanning electron microscopy (SEM). The working distance was 10 mm; ETD and CBS detectors were used for secondary and back-scattered electrons, respectively; elemental analysis was performed by EDS.

The Ni<sup>0</sup>/CER catalyst in a wet form was loaded in a flow reactor and dried to remove water in a flow of H<sub>2</sub> at a temperature of 120°C for 0.5 h. The catalyst in the reactor was placed between the layers of quartz glass as an inert packing material. Hydrogen was dried in a BiGasCleaner laboratory system for gas cleaning and drying, which consisted of two tandem columns packed with silica gel and activated carbon. After drying in the flow of H<sub>2</sub>, dicyclopentadiene and hydrogen were continuously supplied to the catalyst in a direct flow from top to bottom at a specified temperature and atmospheric pressure. The temperature in the reaction zone was no higher than 130°C because of the upper limit of the operating temperature of the Purolite CT-175 cation exchange resin [15] and no lower than 80°C for preventing the crystallization of *endo*-tetrahydrodicyclopentadiene.

The conditional residence time of dicyclopentadiene in the catalyst bed ( $\tau$ ) was varied in a range from 18 to 108 s kg<sub>Cat</sub>/mol (where Cat is the catalyst), and the conditional residence time of H<sub>2</sub> in the catalyst bed ( $\tau_{\text{H}_2}$ ) was changed in a range from 5.4 to 36 s kg<sub>Cat</sub>/mol. The molar ratio dicyclopentadiene : H<sub>2</sub> was varied from 1 : 1 to 1 : 8. For studying the effect of temperature on the reaction rate of the hydrogenation of

C=C bonds in dicyclopentadiene, the process was carried out at temperatures of 80–120°C.

The influence of hydrogen absorption by liquid reaction mass on the overall rate of the process was judged from the effect of changes in the conditional residence time of a gas phase in the catalyst bed ( $\tau_{\text{H}_2}$  was varied from 5.4 to 36 s kg<sub>Cat</sub>/mol) on changes in the mole fraction of dicyclopentadiene and its hydrogenation products at constant temperature (80, 90, 100, 110, or 120°C) and dicyclopentadiene feed rate to the reactor (0.0504 mmol/s).

The influence of external diffusion on the apparent rate of the process of dicyclopentadiene hydrogenation was evaluated based on the effect of the flow rate of dicyclopentadiene on changes in the mole fractions of dicyclopentadiene and its hydrogenation products at a constant conditional residence time of reactants in the catalyst bed and the ratio dicyclopentadiene : H<sub>2</sub> = 1 : 4. The catalyst weight was varied in a range of 0.3–1 g, and the feed rate of a liquid phase was changed within the limits of 0.0011–0.0036 mmol/s.

Test samples for analysis were taken directly at the reactor outlet 0.5 h after the beginning of filling a collector for the products of catalysis and placed in individual vessels with the subsequent dissolution in *n*-hexane for analysis by gas–liquid chromatography (GLC). In the parallel testing of reproducibility, the deviation from mean was no higher than 3%.

The quantitative GLC analysis of the reaction mass was carried out on a Kristallyuks-4000M chromatograph (OOO NPF Meta-khrom, Russia) equipped with an HP-5 polar column (0.52 μm × 50 m; active phase, (5% phenyl)-methylpolysiloxane) and a flame-ionization detector (FID). Nitrogen was used as a carrier gas. Cyclohexylamine served as an internal standard. Conditions for the analysis:  $T_i = 100$ –210°C,  $T_{\text{inj}} = 250$ °C, and  $T_{\text{FID}} = 250$ °C.

The material balance was calculated based on the total products of catalysis collected for 1 h of the continuous operation of the setup with consideration for chromatographic data. The calculated balance on carbon showed that the losses of hydrocarbons did not exceed 2 mol %.

## RESULTS AND DISCUSSION

According to the data of scanning electron microscopy (SEM), the size of nickel particles, which form aggregates on the surface of the cation exchange resin, varied from 70 to 150 nm (Fig. 1).

The Ni<sup>0</sup>/CER catalyst exhibited high activity in the reaction of dicyclopentadiene hydrogenation. Thus, the almost complete conversion (97%) was achieved at the molar ratio dicyclopentadiene : H<sub>2</sub> = 1 : 2 and a

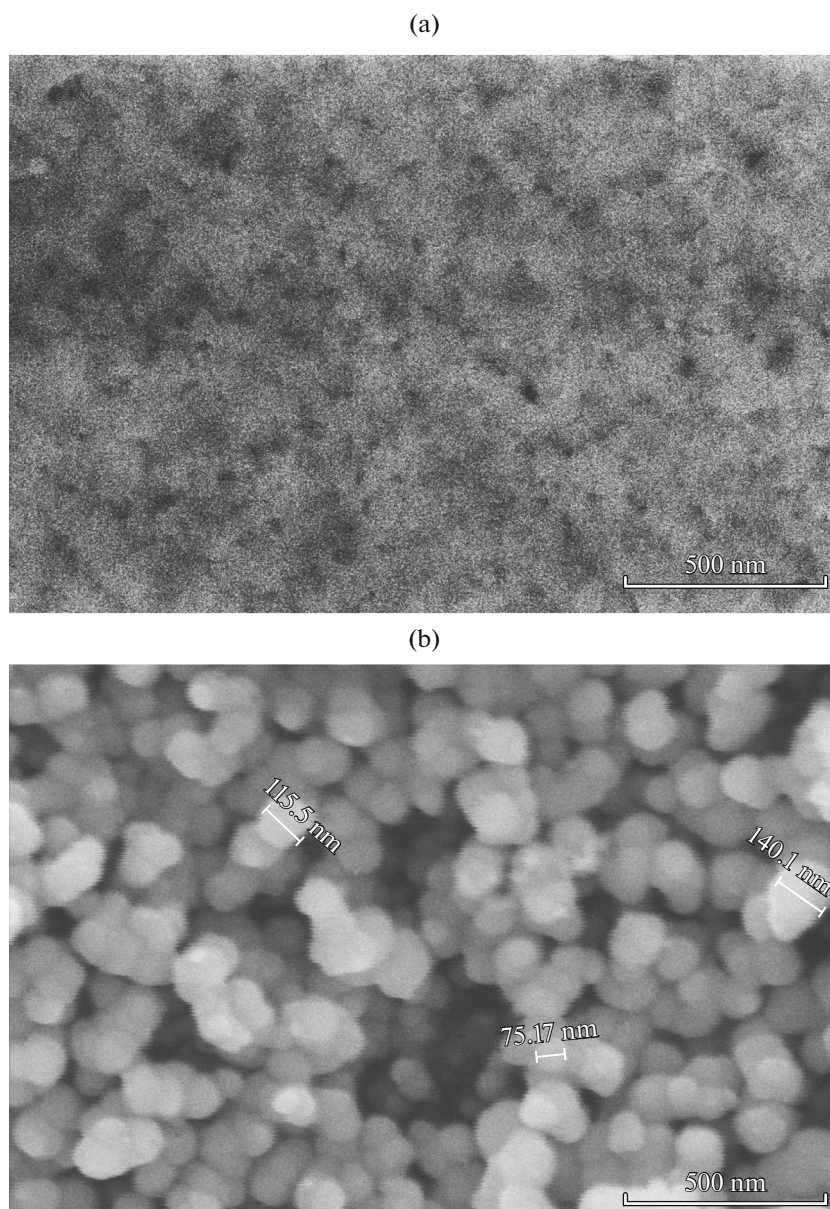


**Fig. 1.** SEM images of (a) the support surface and (b) the surface of the Ni<sup>0</sup>/CER catalyst with specified sizes of separate nickel particles.

temperature of 80°C. The catalyst retained its activity in an excess of hydrogen with respect to dicyclopentadiene of 3 : 1 (a 1.5-fold excess) for 15 h; thereafter, purging with hydrogen for 0.5 h was required for regenerating the catalyst activity.

The hydrogenation of dicyclopentadiene by molecular hydrogen under the process conditions occurs in the three-phase gas (H<sub>2</sub>)–liquid (dicyclopentadiene)–solid (Ni<sup>0</sup>/CER catalyst) system. This process can be represented in more detail as the following several stages:

—the absorption of gaseous hydrogen by liquid reaction mass;

—the diffusion of dissolved hydrogen through a laminar liquid film to the external surface of the Ni<sup>0</sup>/CER catalyst;

—the adsorption of dicyclopentadiene (A) and dissolved hydrogen on the catalyst surface;

—the reaction of dicyclopentadiene (A) hydrogenation with hydrogen on the catalyst surface with the formation of 5,6-dihydrodicyclopentadiene (B);

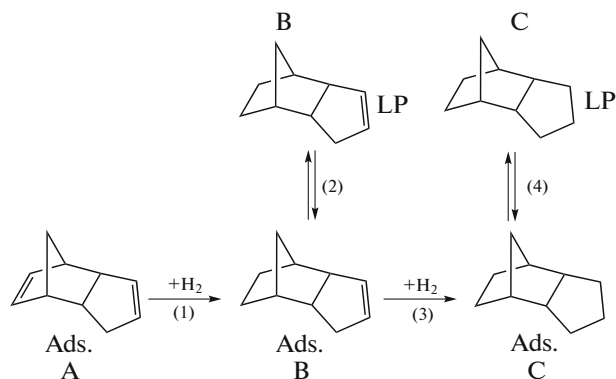
—the reaction of 5,6-dihydrodicyclopentadiene (B) hydrogenation with hydrogen on the catalyst surface with the formation of *endo*-tetrahydrodicyclopentadiene (C) or the desorption of 5,6-dihydrodicyclopentadiene into the liquid phase;

**Table 1.** Apparent reaction kinetic parameters of the hydrogenation of dicyclopentadiene

Reaction	Reaction order with respect to reactants	Apparent rate constant $k_{app}$ , $\times 10^{-3} \text{ L s}^{-1} \text{ kg}_{Cat}^{-1}$					Apparent activation energy $E_a$ , kJ/mol
		temperature, $^{\circ}\text{C}$					
		80	90	100	110	120	
1. $\text{A} + \text{H}_2 \rightarrow \text{B}$	1	$2.43 \pm 0.06$	$3.61 \pm 0.07$	$4.44 \pm 0.12$	$4.93 \pm 0.11$	$5.52 \pm 0.12$	$22.82 \pm 0.99$
2. $\text{B} + \text{H}_2 \rightarrow \text{C}$	1	$9.30 \pm 0.18$	$10.31 \pm 0.25$	$11.08 \pm 0.26$	$11.77 \pm 0.34$	$11.83 \pm 0.14$	$7.18 \pm 0.20$

—the desorption of *endo*-tetrahydrodicyclopentadiene (C) from the catalyst surface.

The processes occurring on the catalyst surface can be represented as the following simplified reaction scheme:



where Ads. and LP refer to adsorption and liquid phase, respectively.

Because it is difficult to construct a complete kinetic model with consideration for not only the adsorption coefficients of substances A, B, and C but also the absorption of gaseous  $\text{H}_2$  by liquid reaction mass and the diffusion of reactants to the catalyst surface at the nearly zero solubility of  $\text{H}_2$  in the liquid phase, the aim of this work was to find the apparent (effective) rate constants of formation of compounds B and C.

On the determination of the influence of the absorption of  $\text{H}_2$  by the liquid reaction mass on the overall rate of the process, we found that the mole fractions of reactants A, B, and C in the reaction system remained constant at  $\tau_{\text{H}_2} = 5.4\text{--}36 \text{ s kg}_{Cat}/\text{mol}$ . This was, apparently, caused by the fact that a constant value of the concentration of  $\text{H}_2$  dissolved in the liquid film was reached for each particular temperature (80, 90, 100, 110, or  $120^{\circ}\text{C}$ ) with the continuous supply of  $\text{H}_2$  into the reactor at  $\tau_{\text{H}_2} \geq 5.4 \text{ s kg}_{Cat}/\text{mol}$ . Thus, the apparent rate of the process depends only on changes in the concentrations of substances A, B, and C on the catalyst surface.

As the flow rate of compound A was changed from 0.0011 to 0.0036 mmol/s at  $\tau = \text{const}$ , the degrees of conversion of compound A at 80, 90, 100, 110, and  $120^{\circ}\text{C}$  had constant values for each temperature. On

the basis of the experimental results, we can hypothesize the absence of the effect of external diffusion in a temperature range of  $80\text{--}120^{\circ}\text{C}$  on the apparent rate of the process at both the first and the second stages of the hydrogenation of compound A on the  $\text{Ni}^0/\text{CER}$  catalyst.

Based on the data obtained and the reaction scheme proposed, we can consider that the consecutive process of the hydrogenation of A to intermediate product B and then to product C on the surface of the  $\text{Ni}^0/\text{CER}$  catalyst can be described by the following system of differential equations:

$$r_1 = dC_A/d\tau = -k_{app1}C_A^n, \quad (1)$$

$$r_2 = dC_B/d\tau = k_{app1}C_A^n - k_{app2}C_B^m, \quad (2)$$

$$r_3 = dC_C/d\tau = k_{app2}C_B^m, \quad (3)$$

where  $r_1$  is the rate of consumption of substance A;  $r_2$  is the rate of change in the concentration of intermediate product B;  $r_3$  is the rate of formation of end product C;  $k_{app1}$  and  $k_{app2}$  are the apparent rate constants of the first and second stages of the process, respectively, which include the concentration of hydrogen on the catalyst surface ( $\text{L s}^{-1} \text{ kg}_{Cat}^{-1}$ );  $C_A$ ,  $C_B$ , and  $C_C$  are the concentration of reactants A, B, and C in the liquid phase, respectively (mol/L);  $\tau$  is the conditional residence time of reactant A in the catalyst bed ( $\text{s kg}_{Cat}/\text{mol}$ ); and  $n$  and  $m$  are the orders of reaction with respect to reactants in the kinetic equation.

In order to confirm this mathematical model, we experimentally studied the functions  $C_A = f(\tau)$ ,  $C_B = f(\tau)$ , and  $C_C = f(\tau)$  at temperatures of 80, 90, 100, 110, and  $120^{\circ}\text{C}$ . The conditional residence time of A ( $\tau$ ) was varied within a range of  $18\text{--}108 \text{ s kg}_{Cat}/\text{mol}$ , other conditions being the same ( $\text{A} : \text{H}_2 = 1 : 4$ , atmospheric pressure).

The processing of the kinetic curves of  $C_A = f(\tau)$ ,  $C_B = f(\tau)$ , and  $C_C = f(\tau)$  with the aid of the Comsol Reaction Engineering Lab 1.5 [17] and Frund [18] software showed that, at  $80\text{--}120^{\circ}\text{C}$ , the experimental data were adequately (error of no higher than 3%) described by equations (1)–(3) with the apparent rate constants of  $k_{app1}$  and  $k_{app2}$  summarized in Table 1.

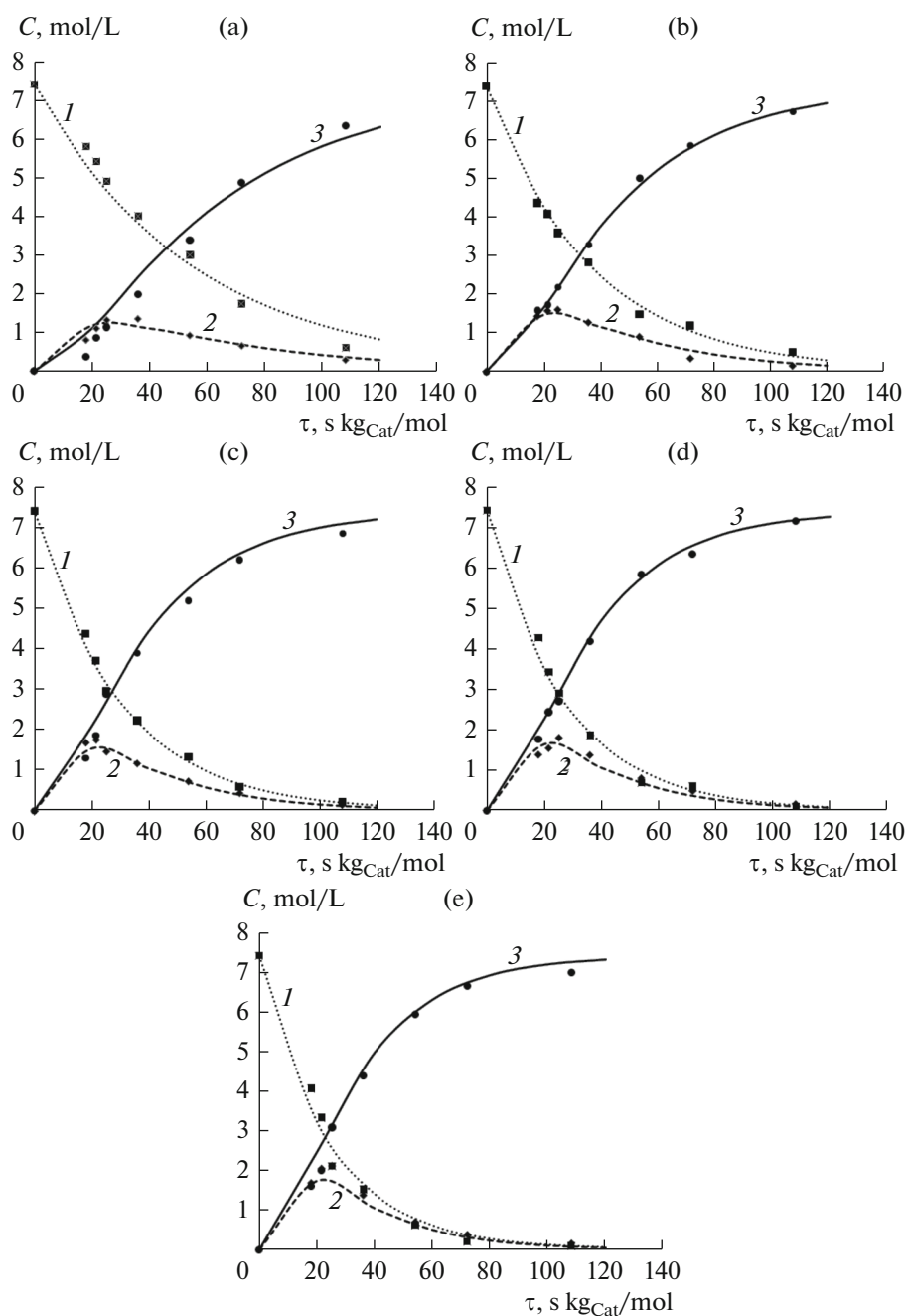


**Fig. 2.** Concentrations of substances (1) A, (2) B, and (3) C as functions of the conditional residence time of liquid phase in the catalyst bed at temperatures of (a) 80, (b) 90, (c) 100, (d) 110, and (e) 120°C. Curves and points refer to the calculated and experimental data, respectively.

Figure 2 compares the experimental data and the kinetic curves constructed according to the mathematical model proposed. Based on the found values of the apparent reaction rate constants, we determined the apparent activation energies for the reactions  $A + H_2 \rightarrow B$  and  $B + H_2 \rightarrow C$  from the graph of the function  $\ln k = f(1/T)$ , which is shown in Fig. 3. Table 1 also summarizes the data obtained.

The effective values of activation energy for the second stage were found lower than those for the first stage. Analogous regularity was described by Skála and Hanika [19], who studied the hydrogenation of dicyclopentadiene on a Pd/C catalyst. Consequently, a more detailed study is required for explaining the smaller value of activation energy for the second stage with respect to the first stage.

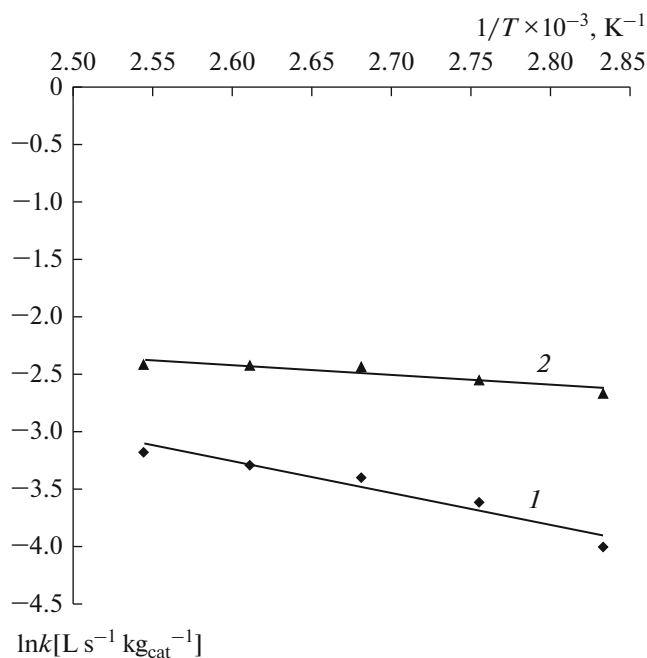


**Fig. 3.** Graph of the function  $\ln k = f(1/T)$  for calculating the activation energies of different stages of the processes (1)  $A + H_2 \rightarrow B$  and (2)  $B + H_2 \rightarrow C$ .

Thus, we were the first to develop a  $Ni^0/CER$  catalyst and to study the reaction kinetics of dicyclopentadiene hydrogenation on the  $Ni^0/CER$  heterogeneous catalyst at atmospheric pressure in a temperature range of 80–120°C. Comparison with published analogs makes it possible to judge prospects for the further study of the catalyst proposed. Thus, for instance, Liu et al. [20] performed the hydrogenation of dicyclopentadiene on  $Pd/Al_2O_3$  in a flow reactor at 120°C and 20 atm with a 98% yield of *endo*-tetrahydrodicyclopentadiene and a productivity of about  $0.38 \text{ kg}_{\text{prod}} \text{ h}^{-1} \text{ kg}_{\text{Cat}}^{-1}$ , whereas the same yield of the product can be reached on the  $Ni^0/CER$  catalyst at 120°C and 1 atm with a productivity of  $4.40 \text{ kg}_{\text{prod}} \text{ h}^{-1} \text{ kg}_{\text{Cat}}^{-1}$ .

The reaction rate equations obtained adequately describe the test process, and they can be used for further study and optimization of the process of dicyclopentadiene hydrogenation.

## REFERENCES

- Claus, M., Claus, E., Claus, P., Hönicke, D., Födisch, R., and Olson, M., *Ullmann's Encyclopedia of Industrial Chemistry*, Wiley, 2016, p. 1. doi 10.1002/14356007.a08\_227.pub2
- Hao, M., Yang, B., Wang, H., Liu, G., Qi, S., Yang, J., Li, Ch., and Lv, J., *J. Phys. Chem. A*, 2010, vol. 114, p. 3811.
- Liu, G., Mi, Z., Wang, L., and Zhang, X., *Ind. Eng. Chem. Res.*, 2005, vol. 44, p. 3846.
- Behr, A., Manz, V., Lux, A., and Ernst, A., *Catal. Lett.*, 2013, vol. 143, p. 241.
- Jacinto, M.J., Landers, R., and Rossi, L.M., *Catal. Commun.*, 2009, vol. 10, p. 1971.
- Ren, Zh., Wang, H.-L., Cai, Y.-Q., Chen, M., and Qian, D.-J., *Mater. Chem. Phys.*, 2011, vol. 127, p. 310.
- Chen, J., Liu, X., and Zhang, F., *Chem. Eng. J.*, 2015, vol. 259, p. 43.
- Abu-Reziq, R., Shenglof, M., Penn, L., Cohen, T., and Blum, J., *J. Mol. Catal. A. Chem.*, 2008, vol. 290, nos. 1–2, p. 30.
- Canning, A.S., Jackson, S.D., Monaghan, A., and Wright, T., *Catal. Today*, 2006, vol. 116, p. 22.
- Marín-Astorga, N., Pecchi, G., Fierro, J.L.G., and Reyes, P., *J. Mol. Catal. A. Chem.*, 2005, vol. 231, nos. 1–2, p. 67.
- Du, W.Q., Rong, Z.M., Liang, Y., Wang, Y., Lu, X.Y., Wang, Y.F., and Lu, L.H., *Chin. Chem. Lett.*, 2012, vol. 23, no. 7, p. 773.
- Cram, D.J. and Allinger, N.L., *J. Am. Chem. Soc.*, 1956, vol. 78, no. 11, p. 2518.
- Chandrasekhar, S., Narsihmulu, Ch., Chandrashekar, G., and Shyamsunder, T., *Tetrahedron Lett.*, 2004, vol. 45, p. 2421.
- Popov, Yu.V., Mokhov, V.M., Nebykov, D.N., Latyshova, S.E., Panov, A.O., Dontsova, A.A., Shirkhanyan, P.M., and Shcherbakova, K.V., *Russ. J. Gen. Chem.*, 2016, vol. 86, no. 12, p. 273.
- Product data sheet Purolite® CT175, 2017. <http://www.purolite.com/product-pdf/ct175?product-Type=regular>.
- Liguori, F., Moreno-Marrodan, C., and Barbaro, P., *Chin. J. Catal.*, 2015, vol. 36, p. 1157.
- Comsol Inc., 2017. <http://www.comsol.ru/chemical-reaction-engineering-module>.
- Frund, Frund, 2015. <http://frund.vstu.ru>.
- Skála, D. and Hanika, J., *Pet. Coal*, 2003, vol. 45, nos. 3–4, p. 105.
- Liu, G., Mi, Z., Wang, L., Zhang, X., and Zhang, S., *Ind. Eng. Chem. Res.*, 2006, vol. 45, p. 8807.

Translated by V. Makhlyarchuk